Lithos 322 (2018) 212–224

Contents lists available at ScienceDirect

Lithos

journal homepage: www.elsevier.com/locate/lithos

Chromium spinel in Late Quaternary volcanic rocks from Kamchatka: Implications for spatial compositional variability of subarc mantle and its oxidation state

Nikolai Nekrylov [a,b,*], Maxim V. Portnyagin [c,d], Vadim S. Kamenetsky [a,e], Nikita L. Mironov [d], Tatiana G. Churikova [f,g], Pavel Yu. Plechov [b], Adam Abersteiner [e], Natalia V. Gorbach [f], Boris N. Gordeychik [a,g], Stepan P. Krasheninnikov [d], Daria P. Tobelko [d], Maria Yu. Shur [h], Sofia A. Tetroeva [h], Anna O. Volynets [f], Kaj Hoernle [c,i], Gerhard Wörner [g]

[a] Institute of Experimental Mineralogy RAS, 142432 Chernogolovka, Russia
[b] Fersman Mineralogical Museum RAS, 119071, Moscow, Russia
[c] GEOMAR Helmholtz Centre for Ocean Research Kiel, 24148, Germany
[d] Vernadsky Institute of Geochemistry and Analytical Chemistry RAS, 119991 Moscow, Russia
[e] Earth Sciences and CODES, University of Tasmania, TAS 7001, Hobart, Australia
[f] Institute of Volcanology and Seismology FEB RAS, 683006, Petropavlovsk-Kamchatsky, Russia
[g] GZG, Abt. Geochemie, Göttingen Universität, 37077 Göttingen, Germany
[h] Lomonosov Moscow State University, Moscow, Russia
[i] Christian-Albrechts Universität zu Kiel, Ludewig-Meyn-Str. 10, 24118 Kiel, Germany

ARTICLE INFO

Article history:
Received 20 July 2018
Accepted 12 October 2018
Available online 17 October 2018

Keywords:
Cr-spinel
Olivine
Kamchatka
Redox conditions
Mantle wedge

ABSTRACT

The Kamchatka volcanic arc (Russia) is one of best-studied, but most complex tectonic margins on Earth, with an extensive geologic history extending back to the Late Cretaceous. Unlike many other subduction zones, primitive basalts with Mg# > 65 are abundant in Kamchatka, thereby allowing characterization of the mantle source through compositional analyses of near-liquidus minerals in the rocks. In this paper, we present a comprehensive dataset on the composition of Cr-spinel inclusions in olivine for all main Late Quaternary volcanic zones in Kamchatka, comprising 1604 analyses of spinel inclusions and their host-olivine in 104 samples from 30 volcanic complexes (single volcanoes and volcanic fields). The studied rocks are basalts, basaltic andesites and high-Mg andesites, which cover the whole compositional range of the primitive Late Quaternary volcanic rocks in Kamchatka. The spinel composition shows large variability. Spinel inclusions with the lowest Cr# and Fe^{3+}/Fe^{2+} ratios were found in basalts from Sredinny Range and Northern Kamchatka, whereas the most Cr-rich and oxidized spinel inclusions occur in basalts and high-Mg andesites from the Central Kamchatka Depression. Intermediate Cr-spinel compositions characterize the Eastern Volcanic Belt of Kamchatka. The compositions of olivine-spinel pairs were used to quantify the oxidation state of parental Kamchatka magmas and the degree of partial mantle melting. The redox conditions recorded in spinel compositions range from $\Delta QFM = +0.7$ to $+3.7$. ΔQFM for spinel from the Sredinny Range and Northern Kamchatka correlates with a number of whole-rock proxies for the involvement of slab-derived components (e.g., La/Nb and Ba/La), which suggests a coupling between mantle oxidation state and slab-derived fluid/melt metasomatism. These correlations were not observed in frontal Kamchatka volcanoes with the highest estimated ΔQFM, which possibly indicates buffering of the mantle oxidation state by sulfur. The estimated degrees of partial mantle melting range from 8 to >20% for Kamchatka volcanoes. Spinel from the Central Kamchatka Depression has the highest Cr# and could crystallize from magmas generated from the most depleted sources. In contrast to the Eastern Volcanic Belt, spinel Cr# and the inferred degrees of melting in the Central Kamchatka Depression do not correlate with spinel TiO_2 content. The apparent decoupling between the proxies of mantle depletion in the CKD spinel is interpreted to reflect refertilization of the CKD mantle by oxidized Ti-rich slab- or mantle lithosphere-derived melts near the northern edge of the subducting Pacific Plate. This study demonstrates that the composition

* Corresponding author at: Institute of Experimental Mineralogy RAS, 142432 Chernogolovka, Russia.
E-mail address: nekrilov.n@gmail.com (N. Nekrylov).

https://doi.org/10.1016/j.lithos.2018.10.011
0024-4937/© 2018 Published by Elsevier B.V.

of Cr-spinel in volcanic rocks in combination with bulk-rock compositions can be a powerful tool to map regional variations of the mantle source depletion, oxidation state, and involvement of various slab-derived components in island-arc magmatism.

© 2018 Published by Elsevier B.V.

1. Introduction

Subduction-related magmatism occurs due to interaction of slab-derived hydrous fluids and melts with the mantle wedge (e.g., Tatsumi and Eggins, 1995). Variations of mantle temperature, depth of melting, composition and flux of slab-derived components cause large compositional heterogeneity in the mantle wedge, which affects the composition of arc magmas and the rheological properties of the mantle (e.g., Ewart et al., 1998; Hirth and Kohlstedt, 2003; Peate et al., 1997; Su et al., 2015). Although studies addressing regional spatial and/or temporal variations of the mantle wedge composition and its oxidation state are rare (e.g., Brounce et al., 2014; Deering et al., 2010), they provide unique insights into the dynamics and evolution of arc systems.

Cr-spinel is a common accessory mineral which occurs in most types of primitive high-Mg volcanic rocks. Due to multicomponent composition, Cr-spinel is considered to be an important petrological indicator of parental magma composition, source fertility and magma oxidation state (e.g., Barnes and Roeder, 2001; Irvine, 1965; Kamenetsky et al., 2001; Leuthold et al., 2015). Magmatic spinel is very sensitive to the composition of equilibrium melt and crystallization conditions, and therefore it can be a powerful tool for discrimination of magmatic rocks from different geodynamic settings (Arai, 1992; Barnes and Roeder, 2001; Kamenetsky et al., 2001). In combination with the compositions of other minerals (e.g., olivine), spinel can be used to quantitatively characterize mantle source depletion (e.g., Arai, 1994) and conditions of crystallization, such as temperature (e.g., Ballhaus et al., 1991; Irvine, 1965; O'Neill and Wall, 1987; Wan et al., 2008) and oxygen fugacity (e.g., Ballhaus et al., 1991; Mattioli and Wood, 1988; O'Neill and Wall, 1987).

In this contribution, we examine the Kamchatka volcanic arc (Russia) located in the northwestern corner of the Pacific Ring of Fire. We present an extensive compositional dataset of spinel inclusions hosted in high-Mg olivine from mafic volcanic rocks in order to characterize the compositional variability and oxidation state of the mantle beneath Kamchatka. Our results demonstrate that subduction-related processes have a strong influence on the oxidation state of subarc mantle. Furthermore, we suggest that there were large variations in the degree of partial mantle melting, which could have been previously underestimated, based solely on fluid-immobile incompatible element systematics in magmas.

2. Geological setting and samples

The Kamchatka volcanic arc is located in the northwestern corner of the Pacific Ring of Fire. It is connected with the Kurile volcanic arc along its southern margin and connects at a nearly right angle with the Aleutian Arc in the north. Quaternary volcanism in Kamchatka takes place in response to subduction of the Pacific oceanic plate under the Eurasian continental margin (e.g., Gorbatov et al., 1997). The Pacific plate is currently subducting under the southern and central parts of Kamchatka at a rate of ~8 cm/yr (Demets et al., 1990). At the Kamchatka-Aleutian arc junction, the subduction trench terminates at approximately 55°N, however, no geophysical constraints on the subducted plate have been produced for north Kamchatka (Levin et al., 2002).

The geological history of Kamchatka extends into the Late Cretaceous and includes numerous episodes of terrane accretion, stretching and in-situ, subduction-related volcanism (Avdeiko et al., 2007; Lander and Shapiro, 2007). According to Lander and Shapiro (2007), Kamchatka is comprised of two major volcanic belts: i) the Eastern Kamchatka Volcanic Belt, and ii) Central Kamchatka Volcanic Belt (Fig. 1). The Wadati-Benioff zone is located at 90–200 km depth beneath the Eastern Kamchatka Volcanic Belt and at >300 km depth under the southern part of Central Kamchatka Volcanic Belt (Gorbatov et al., 1997; Zhao et al., 2010). The Eastern Kamchatka Volcanic Belt hosts some of the most active volcanoes in the world, as well as numerous volcanic fields of monogenetic cinder cones and associated lavas. The belt includes three major segments, which are distinct in age of volcanism, spatial distribution of volcanoes and rock composition: i) southern segment or South Kamchatka (SK; ~51.1°–52.9° N), ii) central segment or Eastern Volcanic Front (EVF; ~52.9°–55.3° N), and iii) northern segment, which includes volcanoes of the Central Kamchatka Depression (CKD; ~55.3–57.4° N). The SK segment is the continuation of the Northern Kurile Arc and has been volcanically active since the Late Eocene. The central (EVF) and northern (CKD) segments have been established more recently, beginning from the Late Miocene (EVF) to Quaternary (CKD) (Lander and Shapiro, 2007). The central and northern segments formed in response to an echelon accretion of Shipunsky, Kronotsky and Kamchatsky (collectively called 'Eastern') Peninsulas in Kamchatka (Fig. 1). The accretion propagated from south to north, resulting in the eastward migration of volcanism in respect to the Central Kamchatka Volcanic Belt (e.g., Avdeiko et al., 2007; Lander and Shapiro, 2007; Park et al., 2002). The Central Kamchatka Volcanic Belt, consisting of the Sredinny Mountain Range (SR), is formed by numerous historically inactive polygenetic volcanoes, monogenetic cones and related lava fields (Churikova et al., 2001; Ponomareva et al., 2007; Volynets et al., 2010). Quaternary volcanism in North Kamchatka is represented by a chain of extinct volcanoes and fields of monogenetic cones extending from Nachikinsky volcano on Ozernoy Peninsula in the northernmost CKD towards the Sredinny Range. This volcanism is not related to modern subduction, but formed due to decompression mantle melting, possibly following slab break-off under this region (Levin et al., 2002; Portnyagin et al., 2005a, 2007a). In this work we refer to this particular region as North Kamchatka (NK), not to be confused with the northern segment (CKD) of the Eastern Kamchatka Volcanic Belt.

We studied the composition of Cr-spinel inclusions in olivine crystals from 104 samples. The samples were collected from 30 volcanoes and volcanic fields, including all the main late Quaternary volcanic zones of Kamchatka (Fig. 1): SK (Bol'shaya Ipel'ka, Savan River, Asacha, Opala, Tolmachev Dol volcanic field, Tolmachev, Mutnovsky, Gorely, Barkhatnaya Sopka), EVF (Avachinsky, Zhupanovsky, Bakening, Karymsky, Schmidt, Gamchen, Komarov), CKD (Tolbachik, Kamen, Klyuchevskaya Sopka, Ploskie Sopki volcanic massif, Kharchinsky, Zarechny, Shiveluch, Shisheisky Complex), SR (Ichinsky, Akhtang, Kekuknaisky volcanic field, Sedanka volcanic field, Tobeltsen) and NK (Nachikinsky). Bulk-rock compositions for most samples were previously reported (Bindeman et al., 2005; Churikova et al., 2001, 2013; Dirksen and Melekestsev, 1999; Dorendorf et al., 2000a; Duggen et al., 2007; Gorbach et al., 2013; Gorbach and Portnyagin, 2011; Grib and Perepelov, 2008; Plechova et al., 2011; Portnyagin et al., 2005a, 2005b, 2007b, 2015; O. Volynets, 1994; O. Volynets et al., 2000; A. Volynets et al., 2010). The host rocks have MgO > 4 wt%, Mg# > 0.46 and represent the entire range of primitive to moderately fractionated rock compositions from Kamchatka (Fig. 2). The majority of the rocks are basalts,

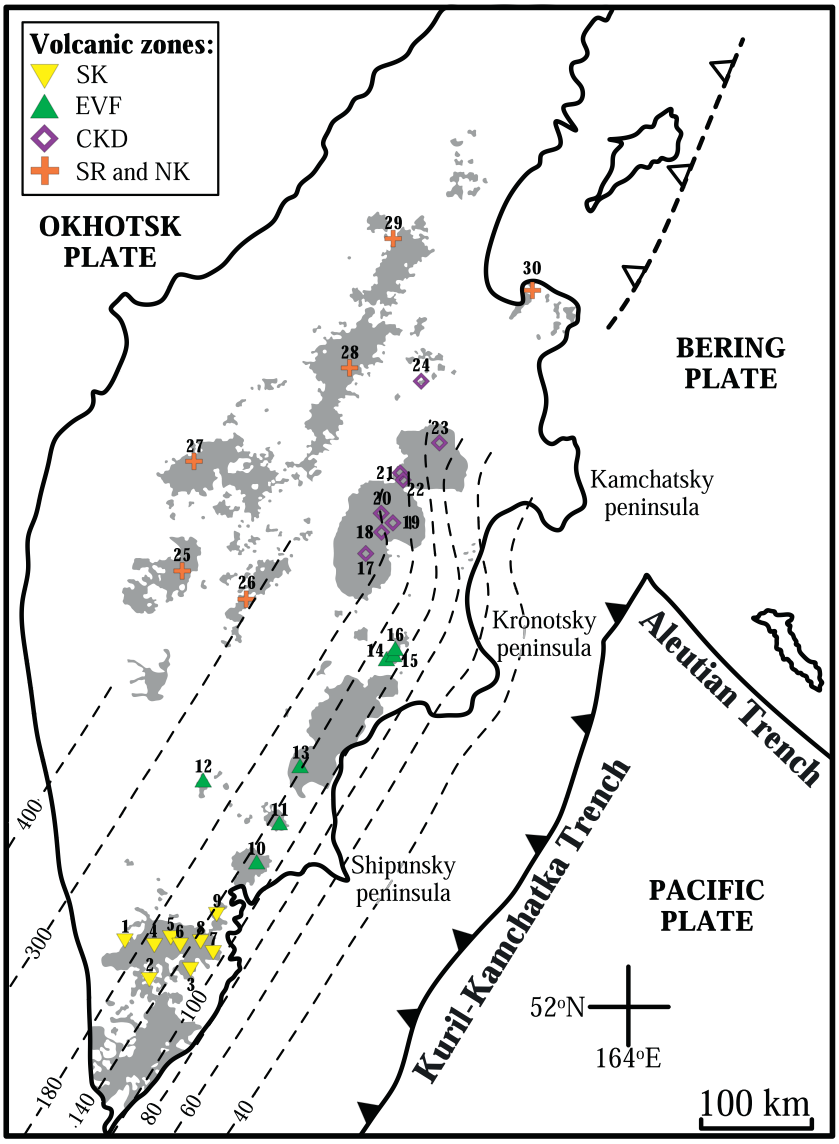

Fig. 1. Map of late Quaternary volcanism in Kamchatka. The distribution of late Quaternary volcanic rocks is shown by grey fields (Ponomareva et al., 2007). Dashed lines mark the depth of the Wadati-Benioff zone (Gorbatov et al., 1997). Numbers indicate volcanoes and volcanic fields in the areas of South Kamchatka (1–9), Eastern Volcanic Front (10–16), Central Kamchatka Depression (17–24), Sredinny Range (25–29) and Northern Kamchatka (30) which were studied in our work: 1 – Bol'shaya Ipel'ka; 2 – Savan River; 3 – Asacha; 4 – Opala; 5 – Tolmachev Dol volcanic field; 6 – Tolmachev; 7 – Mutnovsky; 8 – Gorely; 9 – Barkhatnaya Sopka; 10 – Avachinsky; 11 – Zhupanovsky; 12 – Bakening; 13 – Karymsky; 14 – Schmidt; 15 – Gamchen; 16 – Komarov; 17 – Tolbachik; 18 – Kamen; 19 – Klyuchevskaya Sopka; 20 – Ploskie Sopki volcanic massif; 21 – Harchinsky; 22 – Zarechny; 23 – Shiveluch; 24 – Shisheisky complex; 25 – Ichinsky; 26 – Akhtang; 27 – Kekuknaisky volcanic field; 28 – Sedanka volcanic field; 29 – Tobeltsen; 30 – Nachikinsky.

basaltic andesites and high-Mg andesites of the medium-K subalkaline series. Low-K basalts (3 samples) are from Avachinsky and Mutnovsky volcanoes, and high-K basalts (7 samples) are from Bolshaya Ipel'ka, Tolbachik and Shiveluch volcanoes. High-K basaltic trachyandesites are from Nachikinsky volcano in NK. The bulk-rock compositions are presented in Supplementary Table 1.

3. Dataset and analytical methods

The dataset comprising of ~2000 analyses of olivine-hosted spinel inclusions and their host olivine grains was collected in several laboratories over the last 20 years. The majority of the data was obtained at GEOMAR (Kiel) using a Cameca SX50 (until 2007) and JEOL JXA8200 (2007–present) and in GZG (Geochemisches Institut, Göttingen) using a JEOL JXA 8900RL. Standardization and quality control in the GEOMAR lab was carried out using common reference materials: chromite NMNH117075, ilmenite NMNH96189 and olivine NMNH111312–44 (Jarosewich et al., 1980). The analyses were performed at 15 kV accelerating voltage, 20 nA for spinels and 20, 100 or 300 nA for olivine. Typical on-peak counting time was 20s for all elements. Some recent analyses of olivine were performed at 300 nA and 100–300 s counting time for trace elements (Al, Mn, Ni, Ca, Cr). For standardization of major and trace elements in spinel and olivine, a program in GZG lab used a set of synthetic and natural standards. Peak counting times for major elements were 15–30 s. To ensure accuracy and high precision of olivine analyses and to correct for instrumental drift, we used two San Carlos olivine crystals: USNM 111312/444 (Jarosewich et al., 1980) and commercial San Carlos olivine as "in house" standard crystal SC-Goe (for details see Churikova et al., 2007; Gordeychik et al., 2018). The analyses were performed at 15–20 kV accelerating voltage, 20 nA for spinels, and 300 nA for olivine using 60–300 s counting time for trace elements (Mn, Co, Cr, Ni, Zn, Al, Ca, P) except for two olivine crystals measured at 15 kV and 15 nA using 30 s counting time for Ni.

The remaining analyses were obtained at the Vernadsky Institute, Moscow (Camebax microbeam and Cameca SX-100 operated

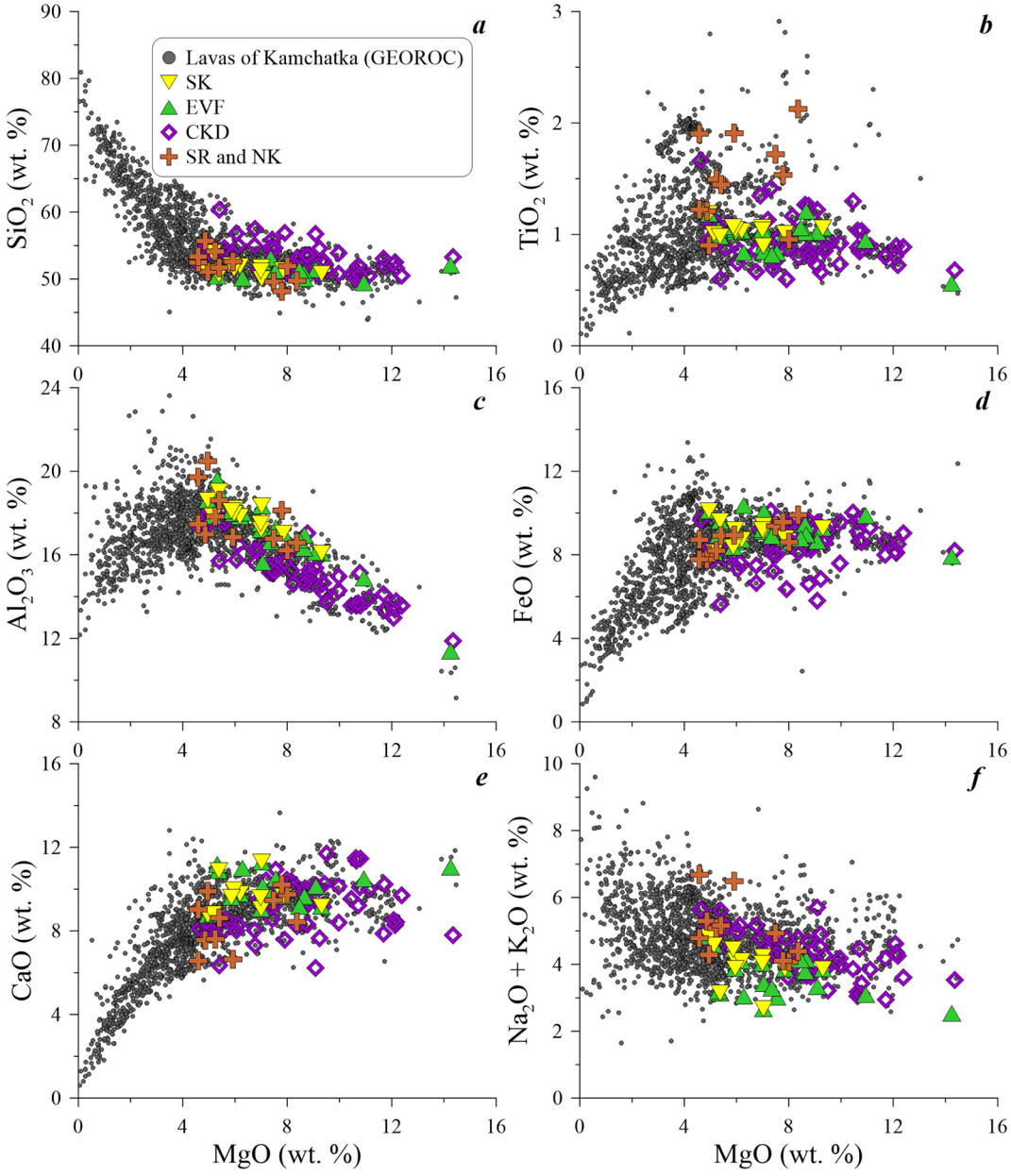

Fig. 2. Bulk-rock composition of studied samples from different volcanic zones of Kamchatka. Data sources are listed in Supplementary Table 1. Volcanic rocks of Kamchatka are shown for comparison (GEOROC database).

at 15 kV, 50 nA) and at the Lomonosov State University, Moscow (EDS CamScan 4DV operated at 15 kV, 1 nA and WDS JEOL JSM-6480 operated at 15 kV, 15 nA). The laboratories are indicated in Supplementary Table 2. Additional information about the analytical techniques can be found in papers devoted to study particular volcanoes in Kamchatka: Avachinsky (Portnyagin et al., 2005b), Zhupanovsky (Plechova et al., 2011), Mutnovsky (Shishkina et al., 2018), Gorely (Nazarova et al., 2017), Karymsky (Tobelko et al., 2019), Klyuchevskoy (Mironov et al., 2015), Shiveluch (Gorbach and Portnyagin, 2011; Gordeychik et al., 2018) and Kekuknaisky (Nekrylov et al., 2018).

The entire dataset was processed to exclude poor quality data and magnetite grains. Analyses containing >1 wt% of SiO_2 were excluded due to contamination by the host olivine. Spinel inclusions, which contain >50 wt% FeO, were also excluded because they represent the late stage magmatic crystallization, which is beyond the scope of this study. The final dataset consists of 1604 olivine-hosted spinel inclusions (Supplementary Table 2): 230 inclusions from 13 samples, coming from 9 volcanoes and volcanic fields of SK; 261 inclusions from 17 samples, taken from 7 volcanoes and volcanic fields of EVF; 904 inclusions from 58 samples, collected from 8 volcanoes and volcanic fields of CKD; 159 inclusions from 13 samples, taken from 5 volcanoes and volcanic fields of SR; 50 inclusions from 3 samples, coming from 1 volcano of NK. A summary of the data is provided in Table 1. Fe^{2+} and Fe^{3+} in spinel were calculated on the basis of ideal spinel stoichiometry as a mixture of ulvöspinel and spinel-type components.

New bulk-rock analyses reported here were performed at the GEOMAR Helmholtz Centre for Ocean Research Kiel, following the method described by Portnyagin et al. (2015). Analyses of AVA-17-06, AVA-17-08 and SHIV-10-24 samples were performed at GZG Göttingen Universität following method described by Churikova et al. (2001).

Table 1
Variations of composition of olivine-hosted Cr-spinel inclusions for each studied volcano.

N on map	Zone	Volcano	Latitude (N)	Longitude (E)	WB zone (km)*	Number of samples	Number of analyses	Host-Olivine (Mg#)	Spinel composition			
									Mg#	Cr#	TiO2	Fe^{2+}/Fe^{3+}
1	SK	Bolshaya Ipelka	52.63	156.97	189	1	2	73.5–75.4	29–33	47–60	0.65–3.2	1.05–1.09
2	SK	Savan VF	52.21	157.28	145	1	19	81.7–86.4	47–59	39–59	0.64–1.24	1.16–1.82
3	SK	Asacha	52.36	157.83	115	1	22	79.2–86.4	39–56	43–52	0.51–0.99	1.35–2.26
4	SK	Opala	52.54	157.34	168	2	23	75.1–86.1	27–54	30–61	0.64–11.8	1.1–2.78
5	SK	Tolmachev Dol VF	52.63	157.58	160	2	33	78.4–85.1	31–60	34–50	0.7–2.79	0.93–1.69
6	SK	Tolmachev	52.55	157.73	160	1	15	77–83.6	34–42	28–45	1.31–2.5	1.15–1.79
7	SK	Mutnovsky	52.45	158.20	107	2	42	74.4–83.7	36–60	21–49	0.52–6.06	0.88–1.9
8	SK	Gorely	52.56	158.03	125	2	52	81.7–86.1	38–67	34–50	0.76–4.22	1.13–1.49
9	SK	Barkhatnaya Sopka	52.80	158.24	130	1	22	78.6–84.8	37–54	41–53	0.91–3.15	1.0–1.38
10	EVF	Avachinsky	53.26	158.84	120	6	103	76.9–91.2	26–64	32–82	0.25–8	0.8–2.75
11	EVF	Zhupanovsky	53.59	159.15	122	2	8	76–81	36–43	34–47	1.19–1.67	0.92–1.1
12	EVF	Bakening	53.91	158.07	208	3	59	77.5–88.5	46–68	3–56	0.3–2.9	0.77–1.93
13	EVF	Karymsky	54.05	159.44	134	3	47	82.5–91.4	42–61	49–79	0.27–1.23	1.11–2.71
14	EVF	Schmidt	54.92	160.63	110	1	17	82.1–89.7	32–60	24–66	0.32–1.15	1.67–2.59
15	EVF	Gamchen	54.97	160.70	109	1	1	89.3	62.0	58.0	0.48	2.23
16	EVF	Komarov	55.03	160.73	110	1	26	75.6–89.2	32–67	35–59	0.43–0.84	1.14–3.45
17	CKD	Tolbachik	55.83	160.33	190	12	255	76.5–92	32–75	15–78	0.08–5.72	0.77–2.75
18	CKD	Kamen	56.02	160.59	170	1	2	71.7–72.1	52–54	1–3	1.02–1.4	2.04–2.26
19	CKD	Klyuchevskoy	56.06	160.64	165	7	145	77.8–91.3	24–65	38–82	0.1–6.95	1.09–4.42
20	CKD	Ploskie Sopki	56.11	160.51	180	1	2	84.1–89.5	35–60	61–82	0.48–6.95	1.13–2.13
21	CKD	Kharchinsky	56.43	160.83	140	11	74	81.1–91.3	29–71	10–79	0.39–1.61	0.64–2.7
22	CKD	Zarechniy	56.38	160.83	140	4	34	81.6–91.2	27–63	63–79	0.38–2.23	1.26–2.72
23	CKD	Shiveluch	56.65	161.36	90	16	357	75.6–92.5	29–67	37–85	0.22–3.73	0.87–3.86
24	CKD	Shisheisky	57.15	161.08	120	6	35	78.5–90.6	24–64	1–83	0.15–4.09	0.87–3.04
25	SR	Ichinsky	55.68	157.72	400	5	49	78–87	32–64	7–59	0.33–4	0.97–7.22
26	SR	Akhtang	55.43	158.65	300	1	48	80.8–87.1	35–60	44–68	0.37–1.97	1.03–2.45
27	SR	Kekuknaisky VF	56.56	157.95	–	1	14	81.4–83.5	62–67	17–22	0.59–0.83	1.92–2.23
28	SR	Sedanka VF	57.27	160.08	–	5	41	79.4–84.9	46–70	4–33	0.49–2.56	1.06–1.85
29	SR	Tobeltsen	58.25	160.73	–	1	7	77.3–81	35–47	41–50	1.68–4.49	1.02–1.26
30	NK	Nachikinsky	57.83	162.68	–	3	50	82.3–86.5	42–75	9–56	0.67–2.19	1.85–3.04

Comments: * - depth to Wadati-Benioff zone following Gorbatov et al. (1997).

4. Results

4.1. Composition of host olivine

Composition of olivine grains (Fo = Mg/(Mg + Fe), mol.%) hosting Cr-spinel inclusions in Kamchatka rocks varies from $Fo_{71.7}$ to $Fo_{92.5}$ (Supplementary Table 2; Fig. 3). The most Fo-rich olivine from the different volcanic zones is $Fo_{86.4}$ for SK, $Fo_{91.4}$ for EVF, $Fo_{92.5}$ for CKD, $Fo_{87.1}$ for SR and $Fo_{86.5}$ for NK. Modes of Fo-number, which can be regarded as the characteristic of average degree of magma fractionation, also vary between the zones and correlate with maximum Fo-number determined for each volcanic zone (Fig. 3): $Fo_{84–85}$ for SK, $Fo_{86–87}$ for EVF, $Fo_{88–89}$ for CKD, $Fo_{80–81}$ for SR and $Fo_{84–85}$ for NK. The least magnesian olivine from all volcanic zones has approximately the same composition (Fo_{72}) and corresponds to the appearance of Ti-magnetite, which contains >50 wt% total FeO (Fig. 4a).

4.2. Composition of Cr-spinel inclusions in olivine

The Cr# (Cr/(Cr + Al) × 100, mol.%) of studied spinel inclusions varies from 1.1 to 85.1 (Figs. 4a, c). The majority of spinel inclusions from CKD samples have Cr# = 60–80, whereas only a few samples from other volcanic zones contain spinel with Cr# > 60. Spinel inclusions from SK, SR and NK have Cr# in the range of 20–60. Only spinel inclusions from EVF cover the whole range of Cr# observed in Kamchatka samples. Spinel with high Cr# = 70–80 in EVF were found in samples from the Karymsky volcano and in avachites – exotic picrobasalts from the Avachinsky volcano (Portnyagin et al., 2005b). Mg# of spinel inclusions varies from 25.0 to 76.5 mol%, even within the narrow range of olivine Fo (Fig. 4b). This is because spinel inclusions trapped in olivine grains of narrow compositional range (e.g., $Fo_{84–86}$) exhibit negative correlations between Mg# and Cr# (Supplementary Table 3, Fig. 4d), as expected from strong dependence of the Mg-Fe olivine-spinel partitioning on spinel Cr# (e.g., Kamenetsky et al., 2001). The Mg# of spinel inclusions at given Cr# correlates positively with the Fo-number of host olivine (Fig. 4b). Cation fraction of Fe^{3+} in Kamchatka spinel increases and Fe^{2+}/Fe^{3+} ratio decreases with decreasing host olivine Fo-number (Fig. 4e) without clear distinction between different volcanic zones in Kamchatka.

5. Discussion

5.1. Composition of primitive spinel

In order to assess the composition of primitive olivine-spinel assemblages in Kamchatka rocks, which crystallized from near primary magmas, we filtered our database to exclude spinel hosted by olivine grains with $Fo_{<84}$, which are also strongly enriched in Fe and Ti and approach Ti-magnetite composition. The remaining spinel inclusions in olivine $Fo_{84–92.5}$ are present in our dataset for 27 out of 30 volcanoes from all volcanic zones in Kamchatka (449 inclusions from 79 samples). Spinel inclusions in olivine with $Fo_{>84}$, which crystallized from near primary or slightly fractionated magmas, are referred to hereafter as 'primitive spinel'. Significant parts of this dataset comprise spinel trapped in olivine with $Fo_{>88}$, which could crystallize from near *primary* mantle-derived magmas. However, high-Fo olivine was not found in all volcanic zones, thereby hampering comparisons with regards to spinel composition. The compositions of the primitive spinel trapped by the most Mg-rich olivine from every sample were averaged and together with their host rock composition are presented in Supplementary Table 4.

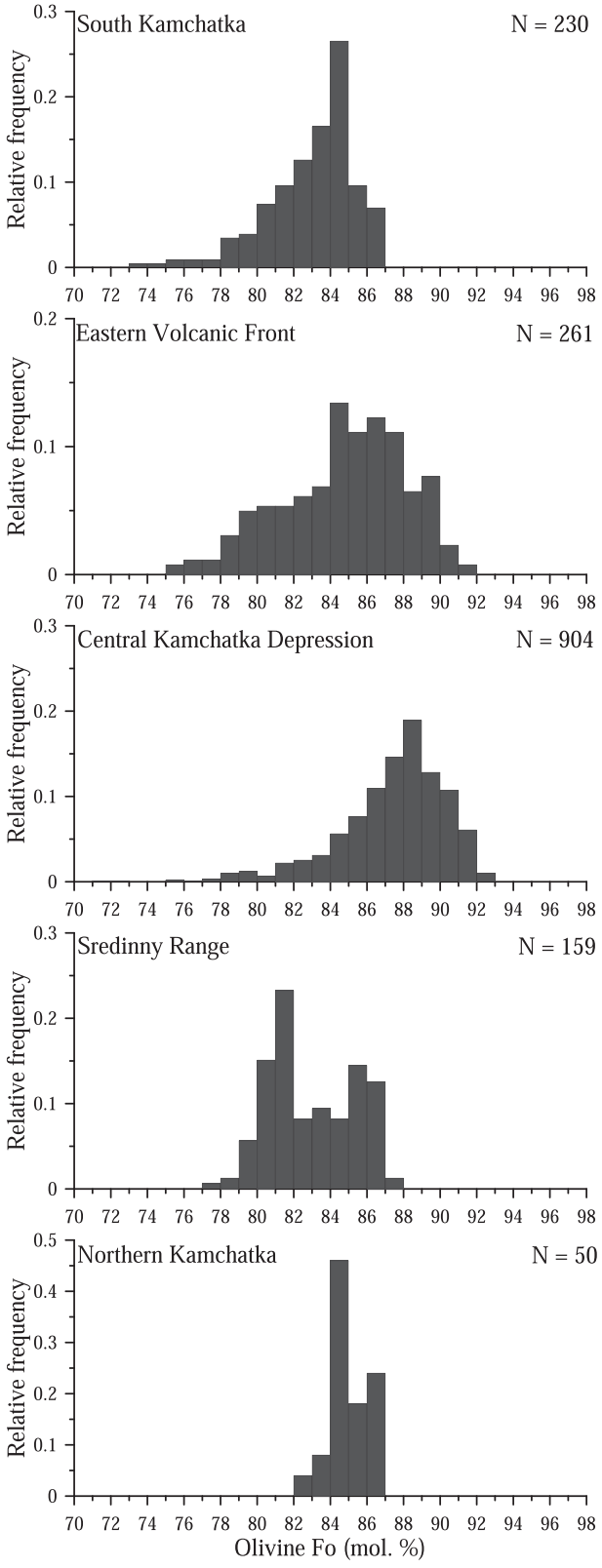

Fig. 3. Histograms of host-olivine Fo-number for different volcanic zones of Kamchatka. N is the number of analyses.

Cr# in primitive spinel from Kamchatka varies from 21.0 to 79.7 (Fig. 5a), which can be caused either by fractionation of Cr-rich phases, such as high-Ca pyroxene and Cr-spinel (Smith and Leeman, 2005) or by compositional variations in parental magmas and their sources, due to variations of Cr/Al ratio (Arai, 1994; Dick and Bullen, 1984). As illustrated in Fig. 4c, Cr# in spinel from for example the CKD volcanoes, where olivine phenocrysts have full range of compositions from $Fo_{92.5}$ to Fo_{72}, does not correlate systematically with the Fo-number of the host olivine. Based on this observation, we conclude that Cr# in Kamchatka spinel is not significantly affected by fractionation of pyroxene and spinel, which typically accompany olivine during the early stages of crystallization of primitive Kamchatka magmas (e.g., Bergal-Kuvikas et al., 2017; Portnyagin et al., 2015). Thus, the variations in primitive spinel Cr# between different samples and volcanic zones in Kamchatka are likely related to variability of the primary melt compositions and their mantle sources.

Direct comparison of the composition of primitive spinel inclusions and the composition of their host rocks provides additional evidence of a close relationship between them. Kamenetsky et al. (2001) showed that Al_2O_3 content in primitive spinel correlates strongly with Al_2O_3 contents in equilibrium melt. In our case, we compared Al_2O_3 content of spinels with the bulk host rock Al_2O_3 content (Fig. 5d). Despite some scatter, a correlation is evident between Al_2O_3 content in spinel and in host rocks. The trend is comparable to that proposed by Kamenetsky et al. (2001), but shows elevated Al_2O_3 in the bulk host rocks. A possible reason for the descrepancy with published data may be that the studied rocks are typically more evolved than melts in equilibrium with $Fo_{>84}$ and therefore likely have higher Al_2O_3 than the melts, from which primitive assemblages of olivine and spinel were crystallized. In contrast, Kamenetsky et al. (2001) used compositions of melt inclusions in spinel to constrain this correlation, which better represent equilibrium melt compositions. Additional evidence of compositional links between the host rocks and spinel is shown by correlating their TiO_2 contents (Fig. 5e). The apparent Ti partitioning is similar to that reported for other suites of magmatic spinel (Kamenetsky et al., 2001). The correlation of Al_2O_3 and TiO_2 in spinel and their host rocks shows that spinel crystallized from melts, which were compositionally similar to the bulk-rock composition. Therefore, the major and trace element compositions of the host rocks can be used to further evaluate major controls on spinel compositions (see sections 5.2, 5.3 and 5.4).

Kamenetsky et al. (2001) proposed using a TiO_2 vs. Al_2O_3 diagram for primitive spinel compositions in olivine Fo > 84 to discriminate between geodynamic setting. In this diagram, compositions of spinel from Kamchatka fall into the fields of arc basalts (CKD and EVF) and MORBs (SK, EVF, SR and NK) (Fig. 5f). In some samples, the MORB-like compositions of spinel can be explained by their back-arc origin (Kamenetsky et al., 2001). Spinel from SK and EVF are from volcanic front volcanoes in Kamchatka. Based on this data, the compositional field of island-arc spinel proposed by Kamenetsky et al. (2001) should be extended to include part of the field of spinel from MORBs. The occurrence of low Cr# spinel in typical arc rocks, like those from the Kamchatka arc front volcanoes (SK, EVF), was also noted by Smith and Leeman (2005). A more robust criterion to distinguish spinel from arc and mid-ocean ridge settings is by comparing their different oxidation states. Low Cr# spinel from SK and EVF are significantly more oxidized in comparison with spinel from MORB, as we show in the following section.

5.2. Oxidation state of primitive Kamchatka magmas and its relation to the host-rock compositions

The occurrence of Fe^{2+} and Fe^{3+} in Cr-spinel renders it one of the best indicators of redox conditions for the upper mantle spinel lherzolites and basaltic magmas (Irvine, 1965), and has been applied in several models of spinel and olivine equilibria (Ballhaus et al., 1991; Mattioli and Wood, 1988; O'Neill and Wall, 1987). To estimate magma oxidation state from the composition of olivine and spinel in this study, we used a model proposed by Ballhaus et al. (1991). This model is sensitive to the presence of orthopyroxene in the liquidus assemblage. Recent studies, however, have shown that this model and

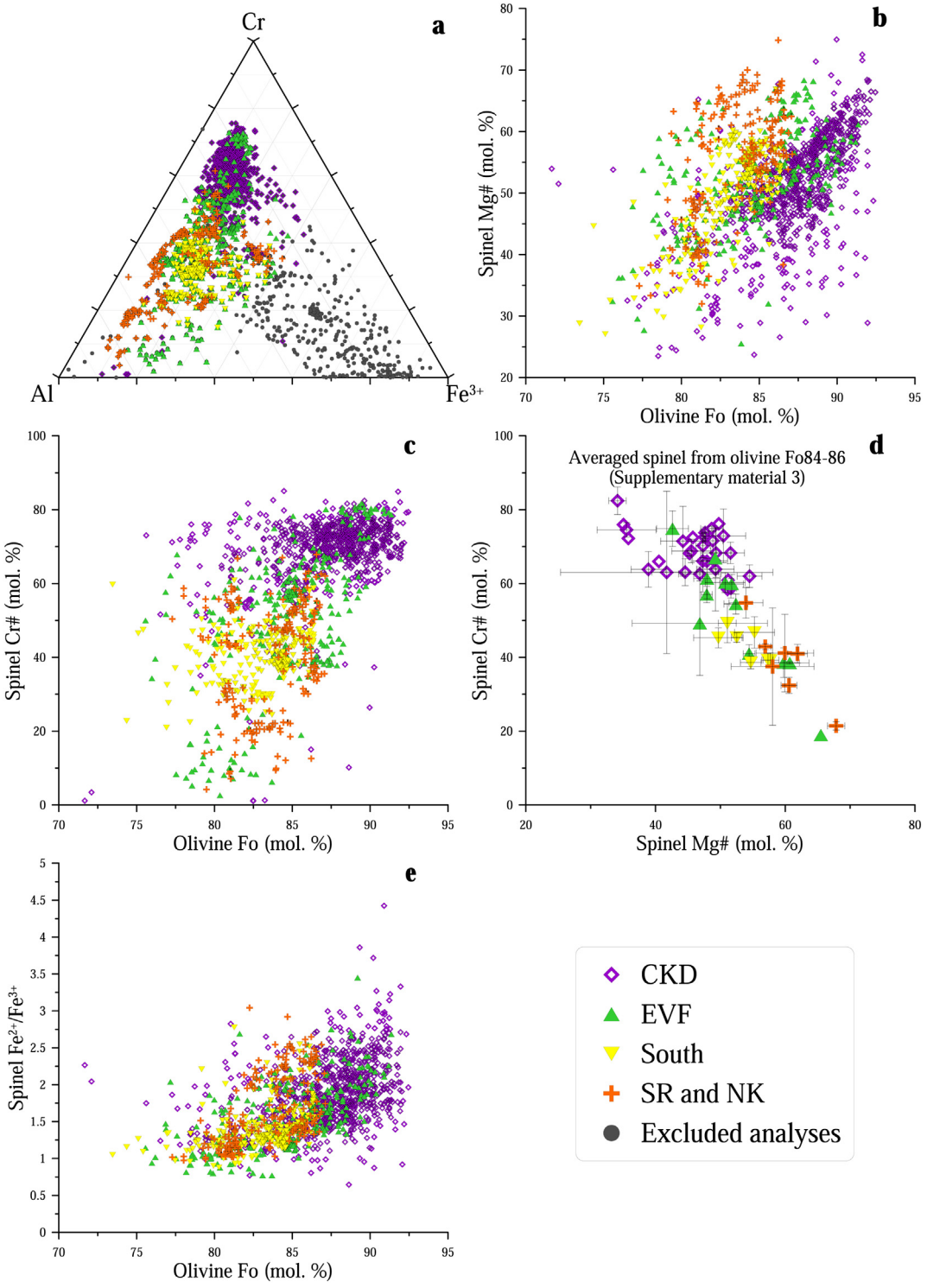

Fig. 4. Composition of Cr-spinel inclusions in olivine from volcanic rocks of Kamchatka. (a) Ternary Al-Cr-Fe^{3+} diagram, (b) spinel Mg# vs. olivine Fo, (c) spinel Cr# vs. olivine Fo, (d) spinel Cr# vs. spinel Mg# averaged by sample for inclusions in olivine $Fo_{84–86}$ (Supplementary Table 3), (e) spinel Fe^{2+}/Fe^{3+} vs. olivine Fo.

oxybarometer based on olivine-melt V partitioning (Nekrylov et al., 2018; Shishkina et al., 2018) yield similar estimates for ΔQFM within 0.5 units (ΔQFM is the deviation of fO_2 from that of quartz-fayalite-magnetite equilibria at given temperature expressed in log. units). Therefore, the model most likely can be applied to primitive and moderately fractionated spinel compositions without correction for magma undersaturation in orthopyroxene. Temperature was calculated using Fe-Mg spinel-olivine equilibrium (Ballhaus et al., 1991). Pressure was assumed to be 0.1 GPa, which corresponds to the upper crustal conditions under Kamchatka. ΔQFM values estimated for different volcanic zones in Kamchatka are 1.7–2.1 (on average 1.9 ± 0.32, 2σ) for SK (except for basaltic cones at Opala caldera with ΔQFM ~ 1.3), 1.1–2.4 (on average 1.61 ± 0.76, 2σ) for EVF, 1.0–3.7 (on average 1.72 ± 0.84, 2σ) for CKD, 1.2–1.7 (on average 1.45 ± 0.44, 2σ) for SR and 0.7–1.1 (on average 0.9 ± 0.44, 2σ) for NK.

Our data shows that primitive Kamchatka magmas are significantly more oxidized compared to MORBs, which typically crystallize at ΔQFM = +0.1 ± 0.2 (Cottrell and Kelley, 2011). Oxidizing conditions,

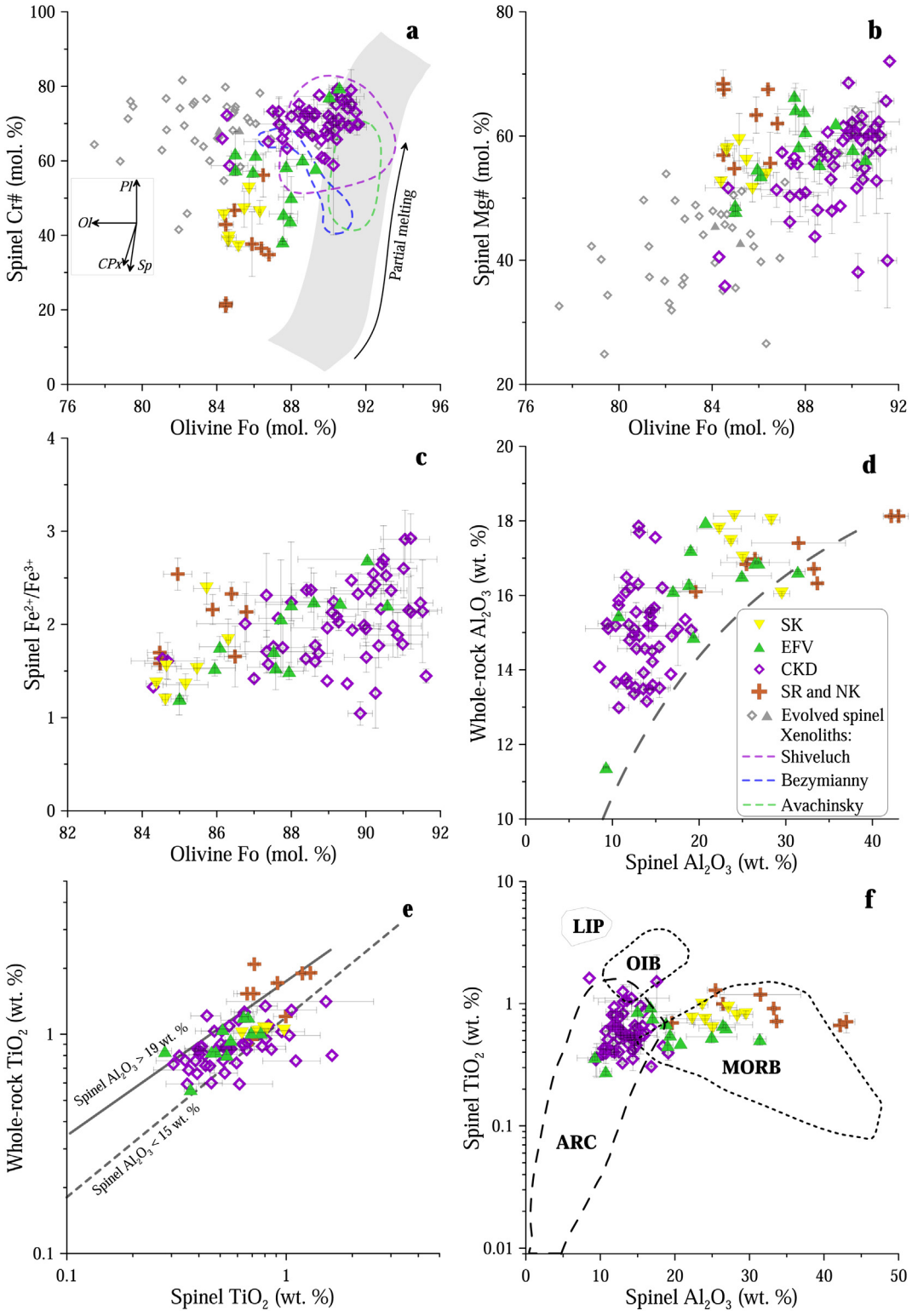

Fig. 5. Average compositions of Cr-spinel inclusions in olivine $Fo_{>84}$ (Supplementary Table 4) from studied samples (Large symbols denote average compositions of coexisting Fo-rich olivine and spinel in one rock sample): (a) Spinel Cr# vs. host-olivine Fo (Grey field indicates Olivine-Spinel Mantle Array (OSMA) after (Arai, 1994)). Dashed lines delineate compositions of coexisting olivine and spinel from mantle xenoliths in Kamchatka volcanic rocks (Bryant et al., 2007; Ionov, 2010; Shcherbakov and Plechov, 2010); (b) Spinel Mg# vs. host-olivine Fo; (c) Spinel Fe^{2+}/Fe^{3+} vs. host-olivine Fo; (d) spinel Al_2O_3 vs. bulk-rock Al_2O_3 content (Grey dashed curve shows equilibrium compositions after Kamenetsky et al. (2001)); (e) Spinel TiO_2 vs. bulk-rock TiO_2 (The dashed and solid grey lines indicate best fit for spinels with Al_2O_3 < 15 wt% and > 19 wt%, respectively (Kamenetsky et al., 2001)); (f) Spinel TiO_2 vs. spinel Al_2O_3 diagram (Fields of typical spinel composition for arcs, MORBs, LIPs and OIBs are after Kamenetsky et al. (2001)). Small grey symbols on figures (a) and (b) show compositions of the most evolved spinel for CKD samples and for 2 samples containing Cr-rich spinel from EVF.

which were estimated for Kamchatka, are typical for arc magmas (ΔQFM from +1 to +2, according to Richards (2015)) and are usually attributed to the transfer of large amounts of ferric iron and other oxidized redox-sensitive elements into the mantle wedge from subducted hydrothermally altered oceanic crust (Evans, 2012; Kelley and Cottrell, 2009). The lowest ΔQFM in Kamchatka was estimated for

SR and NK, where magmas originate from mantle sources with the smallest contribution of subduction-related components (Churikova et al., 2001; Volynets et al., 2010), or by pure pressure-release melting (Portnyagin et al., 2005a).

The dependence of ΔQFM in Kamchatka magmas on the extent of subduction-related metasomatism of their sources is supported by a statistically significant correlation between ΔQFM and indices of slab-derived components, such as La/Nb and Ba/La (e.g., Hanyu et al., 2006; Kelley and Cottrell, 2009), in bulk-rock composition. A particularly strong correlation is observed for samples from SR and NK. The correlation, however, is not significant for EVF, CKD and SK. Nevertheless, the general regional trend of increasing ΔQFM with increasing subduction-related signature in Kamchatka rocks is still evident. This correlation suggests that the oxidation state of Kamchatka magmas and their sources is largely controlled by the amount of slab-derived components that interacted with the mantle wedge and caused coupled mantle oxidation and enrichment in fluid-mobile elements. Similar correlations between Ba/La and melt oxidation state were reported for the Mariana arc (Brounce et al., 2014) and for arc melts in general (Kelley and Cottrell, 2009).

Our data demonstrate that there is no significant difference in the estimated ΔQFM between different zones of the Eastern Kamchatka Volcanic Belt (Supplementary Table 4; Fig. 7a). The ΔQFM estimates, however, are highly variable for CKD volcanoes, especially for those from the northern CKD. These variations are also manifested in the composition of spinel inclusions in olivine with Fo > 88 (Supplementary Table 4), and therefore they cannot be explained by variable magma fractionation and oxidation. Since the minimum value of the estimated ΔQFM for CKD samples is nearly the same as for EVF and SK, these large variations can be caused by an additional oxidizing agent involved in the magma generation beneath the CKD, possibly slab-derived melts (Portnyagin et al., 2007a; Yogodzinski et al., 2001), as discussed in section 5.4.

Some authors have proposed that the contribution of slab-derived components to arc mantle sources decreases from the arc front to the rear arc (e.g., Ishikawa and Nakamura, 1994). We, however, observed no significant correlations between ΔQFM and the depth to the Wadati-Benioff zone beneath a volcano (Fig. 6c). This suggests that the amount of oxidizing slab-derived components may be relatively constant across the Kamchatka Arc, at least in some parts of the arc, where the Wadati-Benioff zone is well defined. This does not contradict the interpretation that the composition of this component changes from relatively trace-element-poor fluid in the volcanic front to trace-element-rich hydrous silicate melt in the rear arc (e.g., Duggen et al., 2007; Portnyagin et al., 2007b).

It is noteworthy that primitive Kamchatka magmas with the highest Ba/La and La/Nb are not oxidized more than ΔQFM = 2 (Supplementary Table 4, Fig. 6). This indicates that their oxidation state may be buffered by some mineral equilibria in the sub-arc mantle under Kamchatka. A possible candidate for such a buffering reaction is the equilibrium between sulfide and sulfate phases, which can coexist at ΔQFM = 0–2 at low pressures and at ΔQFM up to 3.5 at mantle wedge conditions for a wide range of melt compositions (Jugo et al., 2010; Matjuschkin et al., 2016). This reaction can buffer the mantle wedge oxidation state either through oxidation of mantle sulfides by slab-derived fluids (e.g., Brounce et al., 2014), or through reduction of the trisulfur ion (S_3^-) (Pokrovski and Dubrovinsky, 2011) and/or sulfate ion SO_4^{2-} (Bénard et al., 2018) from slab-derived fluids by sulfide precipitation (Rielli et al., 2017).

5.3. Constraints on mantle wedge depletion under Kamchatka from spinel composition

Spinel Cr# is commonly considered a useful indicator of the degree of mantle source depletion in basaltic systems (Arai, 1994; Dick and Bullen, 1984). The Cr/Al ratio in mantle residues and primary melts, as well as in their equilibrium spinel, increases with increasing degree of partial melting of spinel peridotite (e.g., Hellebrand et al., 2001; Jaques and Green, 1980). A direct application of the proposed equations linking Cr# in spinel and degree of mantle melting to volcanic rocks is complicated by significant dependence of the Al partitioning between spinel and melt on pressure (Barnes and Roeder, 2001; Sobolev and Danyushevsky, 1994). The liquidus spinel Cr# does not exactly correspond to spinel Cr# in the residual mantle, when significant differences exist between the pressures of melting and crystallization (Sobolev and Danyushevsky, 1994). This uncertainty decreases with decreasing

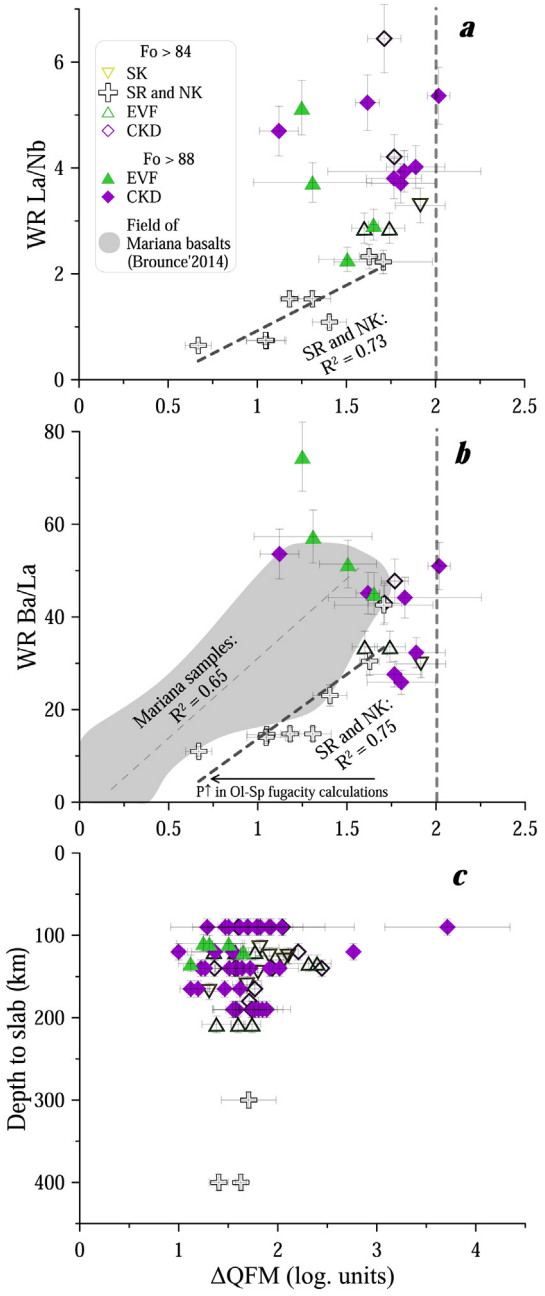

Fig. 6. Redox conditions of magma crystallization estimated from composition of coexisting spinel and olivine (Fo_{84-88} – open symbols; $Fo_{>88}$ – filled symbols (Supplementary Table 4)) in Kamchatka rocks vs. bulk-rock compositions (a, b) and depth from volcano to the Wadati-Benioff zone (c) (Gorbatov et al., 1997). Diagrams (a) and (b) are drawn using ICP-MS trace element data for bulk rocks; low precision XRF data is not shown. Diagram (c) shows data only for those volcanoes where the Wadati-Benioff zone is detected. Vertical dashed lines define ΔQFM = +2 – maximum oxidation level for Kamchatka magmas. The grey field delineates the data from the Mariana Arc (Brounce et al., 2014).

differences between pressure of crystallization and pressure of the last melt equilibrium with mantle peridotite. In conclusion, Cr# of spinel from volcanic rocks is generally informative about maximum degree of melting of the source.

The Cr# of primitive spinel from SK, EVF and CKD closely corresponds to the Cr# of spinel from mantle xenoliths in some Kamchatka volcanic rocks and extends to lower values (Cr# < 40) (Fig. 5a). The mantle xenoliths were described in detail for the Avachinsky (Ionov, 2010), Bezymianny (Shcherbakov and Plechov, 2010) and Shiveluch (Bryant et al., 2007) volcanoes. The majority of them are represented by harzburgites with spinel Cr# = 40–80, which corresponds to more than or equal to 15%, or even in excess of 20%, of near fractional melting to form the residual mantle (Hellebrand et al., 2001; Jaques and Green, 1980). In comparison with spinel in mantle xenoliths, primitive spinel in Kamchatka volcanic rocks has a wider range of Cr# = 20–80, which corresponds to a range of degrees of melting from ~8 to >20%. The lowest degrees of melting (F < 15%) and lherzolite residues (spinel Cr# < 0.4) are predicted for samples from SR, NK and some samples from EVF and SK. Harzburgite residues and F > 15% are typical in most parts of the Eastern Kamchatka Volcanic Belt (SK, EVF, CKD), and the most depleted residues result from the extraction of CKD magmas (Fig. 5a, 7b).

Available data suggest that the parental magmas of Kamchatka volcanoes begin to crystallize in the lower crust at pressures of ~1 GPa (e.g., Gavrilenko et al., 2016; Kersting and Arculus, 1994; Portnyagin et al., 2005b). Assuming that parental melts last equilibrated with mantle peridotite at 2 GPa pressure, the difference in spinel Cr# between mantle residue and magmatic spinel should not exceed 10 mol% (Sobolev and Danyushevsky, 1994). The degrees of melting for Kamchatka mantle source(s), calculated from the model of Hellebrand et al. (2001), can thus be overestimated by 2–3%. This uncertainty is considered to be small and does not significantly exceed the uncertainty related to the spread of spinel Cr# for single rock samples.

Our observations showing significantly higher degrees of partial melting under the Eastern Volcanic Belt, compared to SR and NK, are in general agreement with published data on the composition of mantle xenoliths in Kamchatka rocks and with independent geochemical modeling of bulk-rock and melt inclusion compositions (Churikova et al., 2001; Portnyagin et al., 2007b, 2015). The estimated degrees of mantle melting correlate with decreasing flux of hydrous fluids and melts into the mantle wedge, as the subducting slab under Kamchatka sinks into the mantle and dehydrates. Therefore, the fluid/melt-flux from the subducting slab appears to be the dominant process controlling melting under Kamchatka (Portnyagin et al., 2007b), with possible exceptions in the most northern volcanoes in SR and NK (Portnyagin et al., 2005).

5.4. Evidence for mantle re-fertilization by Ti-rich melts under CKD

Ti is moderately incompatible element during partial melting (Jaques and Green, 1980), and its concentration in primary magmas should provide information on the extent of this process (e.g., Stolper and Newman, 1994). Ti in primitive spinel correlates with melt composition (e.g., Kamenetsky et al., 2001), and therefore it can also be considered as a potential indicator of the mantle depletion and degree of partial melting.

In order to quantitatively estimate the degree of partial mantle melting from Ti content in liquidus spinel, the TiO_2 content in melt derived from Depleted MORB-source Mantle (DMM) and TiO_2 content in spinel in equilibrium with such a melt needs to be calculated. TiO_2 in model partial mantle melts was calculated using the TiO_2 content of enriched DMM (0.132 wt%), bulk partition coefficient (0.058) (Workman and Hart, 2005) and the equation of batch melting (Shaw, 1970):

$$TiO_2^{Melt} = \frac{0.132}{0.058 + F * 0.942} \quad (1)$$

where F is a melt weight fraction.

Using data from Kamenetsky et al. (2001), the dependence of TiO_2 content in spinel on TiO_2 content in melt for island arc basalts can be

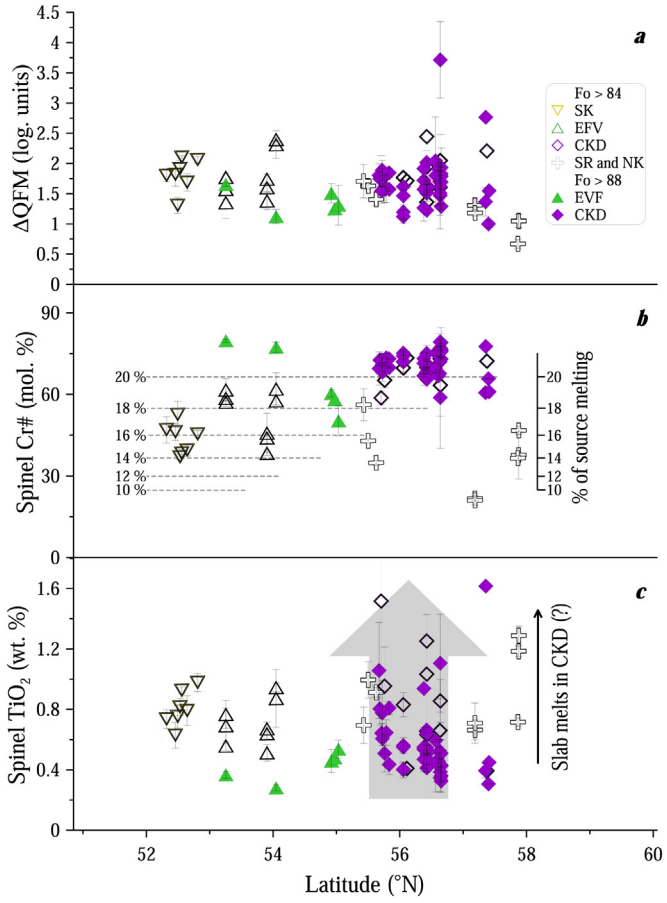

Fig. 7. South to north spatial variability of the estimated redox conditions (a), Cr# (b) and TiO_2 content (c) for spinel hosted in olivine $Fo_{>84}$ (clear symbols) and in olivine $Fo_{>88}$ (filled symbols) (Supplementary Table 4). In plot (b) degrees of mantle melting are shown as a function of spinel Cr# after Hellebrandt et al. (2000).

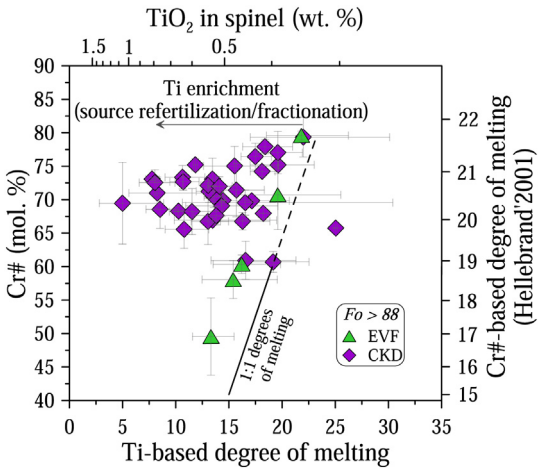

Fig. 8. Degree of melting estimated from TiO_2 content in spinel inclusions in high-Fo olivine ($Fo_{>88}$) vs. their Cr#. The black line marks the 1:1 line for the melting degree estimated from spinel TiO_2 content and from spinel Cr# following the model of Hellebrand et al. (2001). The values of Cr#-based melting degree, corresponding to Cr# > 60, are estimated by extrapolating the 1:1 degree melting line (shown by the dashed line).

expressed as follows:

$$TiO_2^{Sp} = 0.8 * \left(TiO_2^{Melt}\right)^{1.2} \quad (2)$$

By substituting the right side of equation (1) for partial mantle melting for TiO_2^{melt} in equation (2) and re-arranging the resulting equation, it is possible to calculate degree of DMM melting from the equilibrium concentration of TiO_2 in spinel. The resulting equation is:

$$F = -0.06158 + 0.11635 * \left(TiO_2^{sp}\right)^{-0.833} \quad (3)$$

This equation can be used only for spinel in equilibrium with high-Fo olivine (Fo > 88), because of the strong influence of magma fractionation on TiO_2 content in spinel. Spinel in equilibrium with high-Fo olivine in this study only occurs in the EVF and CKD. For the EVF spinel, we found a strong correlation between spinel Cr# and degrees of mantle melting of 16–22% calculated from TiO_2 in spinel using equation {3} (Fig. 8). In contrast, the data for CKD samples are very scattered and did not display any correlation between Cr# and TiO_2 in spinel. A strong correlation for the EVF supports the view that spinel composition can provide information about the degrees of mantle melting, however, data for the CKD do not seem to support this interpretation. The minor discrepancy between the trend of TiO_2-Cr#-based melting degrees for EVF and 1:1 line for these estimations can be explained by the pressure difference between mantle residue and magmatic spinel crystallization, which affects Cr#-based estimations (see Section 5.3).

CKD magmas are clearly anomalous in the Kamchatka arc due to large variations in the estimated ΔQFM, highly variable spinel TiO_2 content and diverse bulk-rock geochemistry (Figs. 6, 7). A number of models have been proposed to explain this abundant and geochemically distinct volcanism in CKD: 1) unusually large flux of hydrous fluids/melts from the subducting Emperor Seamounts (e.g., Churikova et al., 2001; Dorendorf et al., 2000b); 2) slab melting at the Pacific slab edge under the northern CKD (Münker et al., 2004; Yogodzinski et al., 2001) or the entire group of CKD volcanoes (Portnyagin et al., 2007a); 3) interaction of the ascending melts with previously hydrothermally altered lithospheric mantle (Auer et al., 2009; Portnyagin et al., 2007a).

The presently available data does not permit us to fully reconcile the possible influence of these processes on the oxidation and enrichment of the mantle under CKD. It is, however, plausible that the contribution from Ti-rich slab-derived melts can cause re-fertilization of the mantle under CKD or that magmas may be contaminated in the lithospheric mantle during ascent, with both processes potentially causing decoupling between spinel TiO_2 and Cr#. Therefore, care should be taken in estimating the degree of mantle melting of subduction-related magmas based on the widely accepted modeling of fluid-immobile elements in primitive rocks and melt inclusions (Pearce and Parkinson, 1993; Portnyagin et al., 2007b; Stolper and Newman, 1994). Potentially more accurate estimates can be obtained from spinel Cr#, which is not as easily modified in depleted mantle and is not as sensitive to fractional crystallization as TiO_2.

6. Conclusions

We present a comprehensive compositional dataset of 1604 olivine-hosted Cr-spinel inclusions from 104 samples collected from 30 volcanoes from all main late Quaternary volcanic zones in Kamchatka. This data places new constraints on regional variations of the magma oxidation state and the degrees of partial mantle melting under Kamchatka.

1) The oxidation state of parental magmas in Kamchatka varies from ΔQFM = +0.7 to +3.7. For Sredinny Range and Northern Kamchatka ΔQFM correlates with geochemical proxies of slab-derived components, such as Ba/La and La/Nb in the host rocks, and suggests mantle oxidation by slab-derived fluid or melts.
2) The oxidation state of the parental magmas of the Eastern Kamchatka Volcanic Belt varies primarily within the range of ΔQFM = +1 to +2. The lack of correlation between the estimated redox conditions and bulk-rock geochemistry for the active volcanic front in Kamchatka suggests that the mantle oxidation state may be buffered by coexisting sulfide and sulfate phases in the mantle.
3) Variations of primitive spinel Cr# suggest that the degree of mantle melting ranges from 8% to >20% beneath Kamchatka. The least depleted residues were estimated for magmas from the Sredinny Range and Northern Kamchatka, which have the smallest contribution from the subducting slab. Magmas from the Eastern Volcanic Belt and the Central Kamchatka Depression originate by larger degrees of melting, based on high spinel Cr#. However, these magmas are enriched in Ti and can originate from mantle, which was refertilized by slab-derived Ti-rich melts or assimilated such melts from enriched lithospheric mantle beneath Kamchatka.
4) The results of our study demonstrate that the composition of Cr-spinel in volcanic rocks, in combination with bulk-rock compositions, can be a useful tool to map regional variations ofmantle source depletion, oxidation state, and involvement of various slab- or lithosphere-derived components in island-arc magmatism.

Acknowledgements

We are grateful to Daniil V. Popov (University of Geneva) for insightful discussions, Oleg V. Dirksen and Maria M. Pevzner for providing samples. We thank Davide Lenaz and one anonymous reviewer for constructive comments on this manuscript. This study was funded by the Russian Science Foundation grant #16-17-10145 to NN and VSK, German Ministry for Education and Research (BMBF) KOMEX and KALMAR to KH and MP, DFG-RFBR grants # 00-0504000, 16-55-12040 and German Science Foundation grant #Wo362/51-1 to GW and TCH.

Appendix A. Supplementary material

Supplementary data to this article can be found online at https://doi.org/10.1016/j.lithos.2018.10.011.

References

Arai, S., 1992. Chemistry of chromian spinel in volcanic rocks as a potential guide to magma chemistry. Mineral. Mag. 56, 173–184.
Arai, S., 1994. Compositional variation of olivine-chromian spinel in Mg-rich magmas as a guide to their residual spinel peridotites. J. Volcanol. Geotherm. Res. 59, 279–293.
Auer, S.L., Bindeman, I., Wallace, P., Ponomareva, V.V., Portnyagin, M., 2009. The origin of hydrous, high-$\delta^{18}O$ voluminous volcanism: Diverse oxygen isotope values and high magmatic water contents within the volcanic record of Klyuchevskoy volcano, Kamchatka, Russia. Contrib. Mineral. Petrol. 157, 209–230 doi:210.1007/s00410-00008-00330-00410.
Avdeiko, G.P., Savelyev, D.P., Palueva, A.A., Popruzhenko, S.V., 2007. Evolution of the Kurile-Kamchatkan Volcanic Arcs and Dynamics of the Kamchatka-Aleutian Junction. In: Eichelberger, J., Gordeev, E., Izbekov, P., Kasahara, M., Lees, J. (Eds.), Volcanism and Subduction: The Kamchatka Region. American Geophysical Union, pp. 37–55.
Ballhaus, C., Berry, R.F., Green, D.H., 1991. High pressure experimental calibration of the olivine-orthopyroxene-spinel oxygen geobarometer: implications for the oxidation state of the upper mantle. Contrib. Mineral. Petrol. 107, 27–40.
Barnes, S.J., Roeder, P.L., 2001. The range of spinel compositions in terrestrial mafic and ultramafic rocks. J. Petrol. 42, 2279–2302.
Bénard, A., Klimm, K., Woodland, A.B., Arculus, R.J., Wilke, M., Botcharnikov, R.E., Shimizu, N., Nebel, O., Rivard, C., Ionov, D.A., 2018. Oxidising agents in sub-arc mantle melts link slab devolatilisation and arc magmas. Nat. Commun. 9 (1), 3500.
Bergal-Kuvikas, O., Nakagawa, M., Kuritani, T., Muravyev, Y., Malik, N., Klimenko, E., Amma-Miyasaka, M., Matsumoto, A., Shimada, S., 2017. A petrological and geochemical study on time-series samples from Klyuchevskoy volcano, Kamchatka arc. Contrib. Mineral. Petrol. 172, 35.
Bindeman, I.N., Eiler, J.M., Yogodzinski, G.M., Tatsumi, Y., Stern, C.R., Grove, T.L., Portnyagin, M., Hoernle, K., Danyushevsky, L.V., 2005. Oxygen isotope evidence for slab melting in modern and ancient subduction zones. Earth Planet. Sci. Lett. 235, 480–496.
Brounce, M.N., Kelley, K.A., Cottrell, E., 2014. Variations in $Fe^{3+}/\Sigma Fe$ of Mariana arc basalts and mantle wedge fO_2. J. Petrol. 55, 2514–2536.
Bryant, J.A., Yogodzinski, G.M., Churikova, T.G., 2007. Melt-mantle interactions beneath the Kamchatka arc: evidence from ultramafic xenoliths from Shiveluch volcano. Geochem. Geophys. Geosyst. 8.

Churikova, T., Dorendorf, F., Wörner, G., 2001. Sources and fluids in the mantle wedge below Kamchatka, evidence from across-arc geochemical variation. J. Petrol. 42, 1567–1593.

Churikova, T., Wörner, G., Mironov, N., Kronz, A., 2007. Volatile (S, Cl and F) and fluid mobile trace element compositions in melt inclusions: Implications for variable fluid sources across the Kamchatka arc. Contrib. Mineral. Petrol. 154, 217–239.

Churikova, T.G., Gordeychik, B.N., Ivanov, B.V., Wörner, G., 2013. Relationship between Kamen Volcano and the Klyuchevskaya group of volcanoes (Kamchatka). J. Volcanol. Geotherm. Res. 263, 3–21.

Cottrell, E., Kelley, K.A., 2011. The oxidation state of Fe in MORB glasses and the oxygen fugacity of the upper mantle. Earth Planet. Sci. Lett. 305, 270–282.

Deering, C.D., Gravley, D.M., Vogel, T.A., Cole, J.W., Leonard, G.S., 2010. Origins of cold-wet-oxidizing to hot-dry-reducing rhyolite magma cycles and distribution in the Taupo Volcanic Zone, New Zealand. Contrib. Mineral. Petrol. 160, 609–629.

Demets, C., Gordon, R.G., Argus, D.F., Stein, S., 1990. Current plate motions. Geophys. J. Int. 101, 425–478.

Dick, H.J.B., Bullen, T., 1984. Chromian spinel as a petrogenetic indicator in abyssal and alpine-type peridotites and spatially associated lavas. Contrib. Mineral. Petrol. 86, 54–76.

Dirksen, O.V., Melekestsev, I.V., 1999. Chronology, dinamics of formation and eruptive centers morphology of Holocene stage of Avacha river basin areal volcanism (Kamchatka, Russia). Volcanol. Seismol. 1, 3–19 (in russian).

Dorendorf, F., Churikova, T., Koloskov, A., Wörner, G., 2000a. Late Pleistocene to Holocene activity at Bakening volcano and surrounding monogenetic centers (Kamchatka): volcanic geology and geochemical evolution. J. Volcanol. Geotherm. Res. 104, 131–151.

Dorendorf, F., Wiechert, U., Worner, G., 2000b. Hydrated sub-arc mantle: a source for the Kluchevskoy volcano, Kamchatka/Russia. Earth Planet. Sci. Lett. 175, 69–86.

Duggen, S., Portnyagin, M., Baker, J., Ulfbeck, D., Hoernle, K., Garbe-Schönberg, D., Grassineau, N., 2007. Drastic shift in lava geochemistry in the volcanic-front to rear-arc region of the Southern Kamchatkan subduction zone: evidence for the transition from slab surface dehydration to sediment melting. Geochim. Cosmochim. Acta 71, 452–480.

Evans, K.A., 2012. The redox budget of subduction zones. Earth Sci. Rev. 113, 11–32.

Ewart, A., Collerson, K.D., Regelous, M., Wendt, J.I., Niu, Y., 1998. Geochemical evolution within the Tonga-Kermadec-Lau arc-back-arc systems: the role of varying mantle wedge composition in space and time. J. Petrol. 39, 331–368.

Gavrilenko, M., Ozerov, A., Kyle, P.R., Carr, M.J., Nikulin, A., Vidito, C., Danyushevsky, L., 2016. Abrupt transition from fractional crystallization to magma mixing at Gorely volcano (Kamchatka) after caldera collapse. Bull. Volcanol. 78, 47.

Gorbach, N.V., Portnyagin, M.V., 2011. Geology and petrology of the lava complex of Young Shiveluch Volcano, Kamchatka. Petrology 19, 134.

Gorbach, N., Portnyagin, M., Tembrel, I., 2013. Volcanic structure and composition of Old Shiveluch volcano, Kamchatka. J. Volcanol. Geotherm. Res. 263, 193–208.

Gorbatov, A., Kostoglodov, V., Suárez, G., Gordeev, E., 1997. Seismicity and structure of the Kamchatka subduction zone. J. Geophys. Res. B Solid Earth 102, 17883–17898.

Gordeychik, B., Churikova, T., Kronz, A., Sundermeyer, C., Simakin, A., Wörner, G., 2018. Growth of, and diffusion in, olivine in ultra-fast ascending basalt magmas from Shiveluch volcano. Sci. Rep. 8, 11775. https://doi.org/10.1038/s41598-018-30133-1.

Grib, E.N., Perepelov, A.B., 2008. Olivine basalts at the Karymskii Volcanic Center: Mineralogy, petrogenesis, and magma sources. J. Volcanol. Seismol. 2, 228–247.

Hanyu, T., Tatsumi, Y., Nakai, S.I., Chang, Q., Miyazaki, T., Sato, K., Tani, K., Shibata, T., Yoshida, T., 2006. Contribution of slab melting and slab dehydration to magmatism in the NE Japan arc for the last 25 Myr: Constraints from geochemistry. Geochem. Geophys. Geosyst. (8), 7.

Hellebrand, E., Snow, J.E., Dick, H.J.B., Hofmann, A.W., 2001. Coupled major and trace elements as indicators of the extent of melting in mid-ocean-ridge peridotites. Nature 410, 677–681.

Hirth, G., Kohlstedt, D., 2003. Rheology of the Upper Mantle and the Mantle Wedge: a View from the Experimentalists. Inside the Subduc. Factory 83–105.

Ionov, D.A., 2010. Petrology of Mantle Wedge Lithosphere: New Data on Supra-Subduction Zone Peridotite Xenoliths from the Andesitic Avacha Volcano, Kamchatka. J. Petrol. 51, 327–361.

Irvine, T.N., 1965. Chromian spinel as a petrogenetic indicator. Part I. Theory. Can. J. Earth Sci. 2, 648–671.

Ishikawa, T., Nakamura, E., 1994. Origin of the slab component in arc lavas from across-arc variation of B and Pb isotopes. Nature 370, 205.

Jaques, A.L., Green, D.H., 1980. Anhydrous melting of peridotite at 0–15 kb pressure and the genesis of tholeiitic basalts. Contrib. Mineral. Petrol. 73, 287–310.

Jarosewich, E.J., Nelen, J.A., Norberg, J.A., 1980. Reference samples for electron microprobe analysis. Geostand. Newslett. 4, 43–47.

Jugo, P.J., Wilke, M., Botcharnikov, R.E., 2010. Sulfur K-edge XANES analysis of natural and synthetic basaltic glasses: Implications for S speciation and S content as function of oxygen fugacity. Geochim. Cosmochim. Acta 74, 5926–5938.

Kamenetsky, V.S., Crawford, A.J., Meffre, S., 2001. Factors controlling chemistry of magmatic spinel: an empirical study of associated olivine, Cr-spinel and melt inclusions from primitive rocks. J. Petrol. 42, 655–671.

Kelley, K.A., Cottrell, E., 2009. Water and the oxidation state of subduction zone magmas. Science 325, 605–607.

Kersting, A.B., Arculus, R.J., 1994. Klyuchevskoy volcano, Kamchatka, Russia: the role of high-flux recharged, tapped, and fractionated magma chamber(s) in the genesis of high-Al_2O_3 from high-MgO basalt. J. Petrol. 35, 1–41.

Lander, A.V., Shapiro, M.N., 2007. The Origin of the Modern Kamchatka Subduction Zone. In: Eichelberger, J., Gordeev, E., Izbekov, P., Kasahara, M., Lees, J. (Eds.), Volcanism and Subduction: The Kamchatka Region. American Geophysical Union, pp. 57–64.

Leuthold, J., Blundy, J.D., Brooker, R.A., 2015. Experimental petrology constraints on the recycling of mafic cumulate: a focus on Cr-spinel from the Rum Eastern Layered Intrusion, Scotland. Contrib. Mineral. Petrol. 170, 12.

Levin, V., Shapiro, N., Park, J., Ritzwoller, M., 2002. Seismic evidence for catastrophic slab loss beneath Kamchatka. Nature 418, 763.

Matjuschkin, V., Blundy, J.D., Brooker, R.A., 2016. The effect of pressure on Sulphur speciation in mid-to deep-crustal arc magmas and implications for the formation of porphyry copper deposits. Contrib. Mineral. Petrol. 171.

Mattioli, G.S., Wood, B.J., 1988. Magnetite activities across the $MgAl_2O_4$-Fe_3O_4 spinel join, with application to thermobarometric estimates of upper mantle oxygen fugacity. Contrib. Mineral. Petrol. 98, 148–162.

Mironov, N., Portnyagin, M., Botcharnikov, R., Gurenko, A., Hoernle, K., Holtz, F., 2015. Quantification of the CO_2 budget and H_2O–CO_2 systematics in subduction-zone magmas through the experimental hydration of melt inclusions in olivine at high H_2O pressure. Earth Planet. Sci. Lett. 425, 1–11.

Münker, C., Wörner, G., Yogodzinski, G., Churikova, T., 2004. Behaviour of high field strength elements in subduction zones: constraints from Kamchatka-Aleutian arc lavas. Earth Planet. Sci. Lett. 224, 275–293.

Nazarova, D.P., Portnyagin, M.V., Krasheninnikov, S.P., Mironov, N.L., Sobolev, A.V., 2017. Initial H_2O content and conditions of parent magma origin for Gorely volcano (Southern Kamchatka) estimated by trace element thermobarometry. Dokl. Earth Sci. 472, 100–103.

Nekrylov, N., Popov, D., Plechov, P., Shcherbakov, V., Danyushevsky, L., Dirksen, O.V., 2018. Garnet-pyroxenite-derived end-member magma type in Kamchatka: evidence from composition of olivine and olivine-hosted melt inclusions in Holocene rocks of Kekuknaisky volcano. Petrology 26, 329–350.

O'Neill, H.S.C., Wall, V.J., 1987. The olivine-orthopyroxene-spinel oxygen geobarometer, the nickel precipitation curve, and the oxygen fugacity of the Earth's upper mantle. J. Petrol. 28, 1169–1191.

Park, J., Levin, V., Brandon, M., Lees, J., Peyton, V., Gordeev, E., Ozerov, A., 2002. A Dangling Slab, Amplified Arc Volcanism, Mantle Flow and Seismic Anisotropy in the Kamchatka Plate Corner, Plate Boundary Zones. American Geophysical Union, pp. 295–324.

Pearce, J.A., Parkinson, I.J., 1993. Trace element models for mantle melting: application to volcanic arc petrogenesis. Geol. Soc. Lond., Spec. Publ. 76, 373.

Peate, D.W., Pearce, J.A., Hawkesworth, C.J., Colley, H., Edwards, C.M.H., Hirose, K., 1997. Geochemical variations in Vanuatu arc lavas: the role of subducted material and a variable mantle wedge composition. J. Petrol. 38, 1331–1358.

Plechova, A.A., Portnyagin, M.V., Bazanova, L.I., 2011. The origin and evolution of the parental magmas of frontal volcanoes in Kamchatka: evidence from magmatic inclusions in olivine from Zhupanovsky volcano. Geochem. Int. 49, 743.

Pokrovski, G.S., Dubrovinsky, L.S., 2011. The S_3^- ion is stable in geological fluids at elevated temperatures and pressures. Science 331, 1052–1054.

Ponomareva, V.V., Melekestsev, I.V., Braitseva, O.A., Churikova, T., Pevzner, M.M., Sulerzhitsky, L.D., 2007. Late Pleistocene-Holocene Volcanism on the Kamchatka Peninsula, Northwest Pacific Region, Volcanism and Subduction: The Kamchatka Region. pp. 165–198.

Portnyagin, M., Hoernle, K., Avdeiko, G., Hauff, F., Werner, R., Bindeman, I., Uspensky, V., Garbe-Schönberg, D., 2005a. Transition from arc to oceanic magmatism at the Kamchatka-Aleutian junction. Geology 33, 25–28.

Portnyagin, M.V., Plechov, P.Y., Matveev, S.V., Osipenko, A.B., Mironov, N.L., 2005b. Petrology of avachites, high-magnesian basalts of Avachinsky volcano, Kamchatka: I. General characteristics and composition of rocks and minerals. Petrology 13, 99–121.

Portnyagin, M., Bindeman, I., Hoernle, K., Hauff, F., 2007a. Geochemistry of primitive lavas of the Central Kamchatka Depression: magma generation at the edge of the Pacific Plate. In: Eichelberger, J., Gordeev, E., Izbekov, P., Kasahara, M., Lees, J. (Eds.), Volcanism and Subduction: The Kamchatka Region, pp. 199–239.

Portnyagin, M., Hoernle, K., Plechov, P., Mironov, N., Khubunaya, S., 2007b. Constraints on mantle melting and composition and nature of slab components in volcanic arcs from volatiles (H_2O, S, Cl, F) and trace elements in melt inclusions from the Kamchatka Arc. Earth Planet. Sci. Lett. 255, 53–69.

Portnyagin, M., Duggen, S., Hauff, F., Mironov, N., Bindeman, I., Thirlwall, M., Hoernle, K., 2015. Geochemistry of the late Holocene rocks from the Tolbachik volcanic field, Kamchatka: Quantitative modelling of subduction-related open magmatic systems. J. Volcanol. Geotherm. Res. 307, 133–155.

Richards, J.P., 2015. The oxidation state, and sulfur and Cu contents of arc magmas: implications for metallogeny. Lithos 233, 27–45.

Rielli, A., Tomkins, A.G., Nebel, O., Brugger, J., Etschmann, B., Zhong, R., Yaxley, G.M., Paterson, D., 2017. Evidence of sub-arc mantle oxidation by sulphur and carbon. Geochem. Perspect. Lett. 6, 124–132.

Shaw, D.M., 1970. Trace element fractionation during anatexis. Geochim. Cosmochim. Acta 34 (2), 237–243.

Shcherbakov, V.D., Plechov, P.Y., 2010. Petrology of mantle xenoliths in rocks of the Bezymyannyi Volcano (Kamchatka). Dokl. Earth Sci. 434, 1317–1320.

Shishkina, T.A., Portnyagin, M., Botcharnikov, R., Almeev, R.R., Simonyan, D., Garbe-Schonberg, D., Schuth, S., Oeser, M., Holtz, F., 2018. Experimental calibration and implications of olivine-melt vanadium oxybarometry for hydrous basaltic arc magmas. Am. Mineral. 103, 369–383.

Smith, D.R., Leeman, W.P., 2005. Chromian spinel-olivine phase chemistry and the origin of primitive basalts of the southern Washington Cascades. J. Volcanol. Geotherm. Res. 140, 49–66.

Sobolev, A.V., Danyushevsky, L.V., 1994. Petrology and geochemistry of boninites from the north termination of the Tonga Trench: constraints on the generation conditions of primary high-ca boninite magmas. J. Petrol. 35, 1183–1211.

Stolper, E., Newman, S., 1994. The role of water in the petrogenesis of Mariana trough magmas. Earth Planet. Sci. Lett. 121 (3–4), 293–325.

Su, B.X., Teng, F.Z., Hu, Y., Shi, R.D., Zhou, M.F., Zhu, B., Liu, F., Gong, X.-H., Huang, Q.-S., Xiao, Y., Chen, C., He, Y.-S., 2015. Iron and magnesium isotope fractionation in oceanic lithosphere and sub-arc mantle: Perspectives from ophiolites. Earth Planet. Sci. Lett. 430, 523–532.

Tatsumi, Y., Eggins, S., 1995. Subduction zone magmatism. Blackwell Science, Inc. P, p. 211.

Tobelko, D.P., Portnyagin, M., Krasheninnikov, S.P., Grib, E.N., Plechov, P., 2019. Initial H_2O Content and Conditions of Parent Magma Origin for Karymsky Volcano Estimated by Melt Inclusions Study and Trace Element Thermobarometry (Russian Geology and Geophysics In press).

Volynets, O.N., 1994. Geochemical Types, Petrology, and Genesis of Late Cenozoic Volcanic Rocks from the Kurile-Kamchatka Island-Arc System. Int. Geol. Rev. 36, 373–405.

Volynets, O.N., Babanskii, A.D., Gol'tsman, Y.V., 2000. Variations in isotopic and trace-element composition of lavas from volcanoes of the Northern group, Kamchatka, in relation to specific features of subduction. Geochem. Int. 38, 974–989.

Volynets, A.O., Churikova, T.G., Worner, G., Gordeychik, B.N., Layer, P., 2010. Mafic late Miocene-Quaternary volcanic rocks in the Kamchatka back arc region: implications for subduction geometry and slab history at the Pacific-Aleutian junction. Contrib. Mineral. Petrol. 159, 659–687.

Wan, Z.H., Coogan, L.A., Canil, D., 2008. Experimental calibration of aluminum partitioning between olivine and spinel as a geothermometer. Am. Mineral. 93, 1142–1147.

Workman, R.K., Hart, S.R., 2005. Major and trace element composition of the depleted MORB mantle (DMM). Earth Planet. Sci. Lett. 231, 53–72.

Yogodzinski, G.M., Lees, J.M., Churikova, T.G., Dorendorf, F., Wöerner, G., Volynets, O.N., 2001. Geochemical evidence for the melting of subducting oceanic lithosphere at plate edges. Nature 409, 500.

Zhao, D., Pirajno, F., Dobretsov, N.L., Liu, L., 2010. Mantle structure and dynamics under East Russia and adjacent regions. Russ. Geol. Geophys. 51, 925–938.